J. Plasma Physics (2012), *vol.* 78, *part* 5, *pp.* 501–506. © Cambridge University Press 2012
doi:10.1017/S0022377812000104

Resistive wall mode in cylindrical plasmas in the presence of surface currents

SHAOYAN CUI[1], GAIMIN LU[2] and YUE LIU[3]

[1]School of Mathematics and Information, Ludong University, Yantai 264025, China
(shycui@ldu.edu.cn)
[2]Southwestern Institute of Physics, P.O. Box 432, Chengdu 610041, China
[3]Key Laboratory of Materials Modification by Laser, Ion and Electron Beams Ministry of Education, School of Physics and Optoelectronic Technology, Dalian University of Technology, Dalian 116024, China

(Received 13 September 2011; revised 13 December 2011; accepted 24 December 2011; first published online 13 February 2012)

Abstract. Stability of the resistive wall mode in cylindrical plasmas confined by surface currents is investigated for the δ-function and step-function equilibrium surface-current profiles. For the former, it is shown that the perturbations oscillate and even decay for all locations of the initial perturbation. The entire system is stable and the plasma flow has little effect. For the step-function surface-current distribution, it is found that the thicker the surface current layer, the more stable is the system even if the largest initial perturbation is located on the rational surface, but the plasma flow also has little effect on the system.

1. Introduction

The stability of large-scale magnetohydrodynamic (MHD) modes is crucial to the magnetic confinement of toroidal plasmas [1]. In tokamaks, the maximum achievable plasma β (plasma to magnetic pressure ratio) is limited mainly by the low mode number external kink modes [2], which can however be stabilized by a perfectly conducting wall of the plasma confinement device. Nevertheless, the finite resistivity of real conducting walls can convert the stabilized external kink mode into the slowly growing resistive wall mode (RWM) [3–7], which makes the plasma unstable again as well as sets a limit on the plasma β. In order to control the RWM instability, relative rotation between the plasma and the conducting wall and control coil feedback have been proposed [8–18]. On the other hand, rotation of the plasma or wall can lead to a new, flow-driven, resistive wall instability [19–21], which was first considered for the slab geometry [18–20]. It has been shown that the RWM instability can occur when the flow is super-Alfvénic in incompressible plasmas [18, 19] and supersonic in compressible plasmas [19–21].

In the more realistic cylindrical geometry, the RWM instability was considered for a plasma with uniform axial flow and a surface current on the plasma surface using an ideal MHD model [22] in the incompressible limit (*i.e.* the ion acoustic speed $c_s \to \infty$). In this paper, we reconsider the RWM in a compressible, cylindrical plasma with a surface current. In particular, the effect of the thickness of the surface current is investigated.

2. Configuration and initial conditions

Figure 1 shows that the initial plasma state. The plasma has a uniform flow velocity V_0 parallel to the axis and is in a cylinder with radius a. A current sheet is generated at the plasma surface $r = a$. The system is surrounded by a resistive wall with radius b, and the thin wall has a thickness $\delta \ll a,\ b$.

The surface current $\boldsymbol{J}_0$ is parallel to the axis of the cylinder and its thickness can be infinitely small (δ function) as well as finite. Accordingly, for the former case, we have

$$\boldsymbol{J}_0(r) = \hat{z} J_0 a \delta(r-a). \tag{2.1}$$

The magnetic field associated with this surface current is

$$B_\theta(r) = \begin{cases} 0, & 0 \leqslant r < a \\ \dfrac{\mu_0 a^2}{r} J_0, & r \geqslant a. \end{cases} \tag{2.2}$$

A constant axial magnetic field $B_0 = B_{0z}$ is applied. Pressure balanced then requires $(\nabla P)_r = -J_z B_\theta$, or

$$P(r) = \begin{cases} P_0 & 0 \leqslant r < a \\ 0 & r > a, \end{cases} \tag{2.3}$$

where $P_0 = \frac{\mu_0 J_0^2 a^2}{2} = \frac{B_{0\theta}^2(a)}{2\mu_0}$.

We also consider the case when the surface current has a definite thickness, as shown in Fig. 2,

$$\boldsymbol{J}_0 = \begin{cases} \hat{z} J_0 a/\varepsilon, & a-\varepsilon \leqslant r \leqslant a \\ 0, & \text{elsewhere}, \end{cases} \tag{2.4}$$

where $1/\varepsilon \to \delta(r-a)$ as $\varepsilon \to 0$. From the Ampere's law, the magnetic field resulting from this surface current is

$$B_\theta(r) = \begin{cases} 0, & 0 \leqslant r \leqslant a-\varepsilon \\ \mu_0 J_0 \dfrac{a}{\varepsilon}\left[\dfrac{r}{2} - \dfrac{1}{r}\dfrac{(a-\varepsilon)^2}{2}\right], & a-\varepsilon < r \leqslant a \\ \mu_0 J_0 \dfrac{a(2a-\varepsilon)}{2r}, & r > a. \end{cases} \tag{2.5}$$

https://doi.org/10.1017/S0022377812000104 Published online by Cambridge University Press

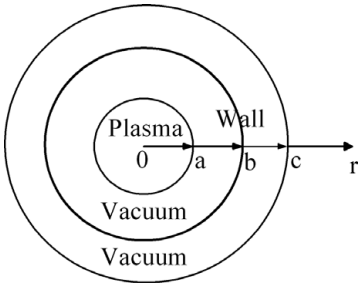


Figure 1. Cross section of the cylindrical plasma model.

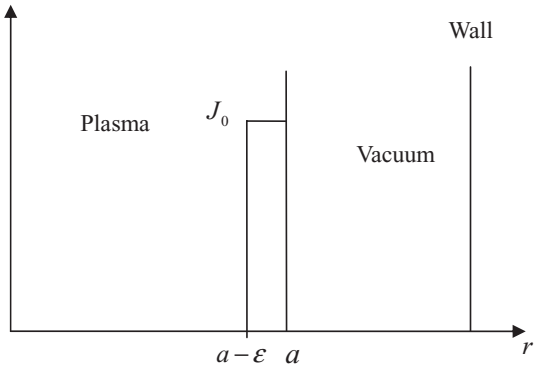


Figure 2. Rectangular radial distribution of the surface current.

Accordingly, from the equilibrium pressure balance we get

$$P(r)=\begin{cases}\bar{P}_0, \\ \bar{P}_0-P_0\dfrac{a^2}{\varepsilon^2}\left[\dfrac{r^2}{2a^2}-\dfrac{(a-\varepsilon)^2}{a^2}\ln\dfrac{r}{a-\varepsilon}-\dfrac{(a-\varepsilon)^2}{2a^2}\right], \\ 0,\end{cases} \tag{2.6}$$

for $0\leqslant r\leqslant a-\varepsilon$, $a-\varepsilon<r\leqslant a$, and $r>a$, respectively.

The boundary condition for the initial state at the plasma-vacuum interface is

$$\left[P(r)+\frac{B_{0\theta}^{p2}}{2\mu_0}\right]_{r=a-0}=\left[\frac{B_{0\theta}^{V2}}{2\mu_0}\right]_{r=a+0}. \tag{2.7}$$

The magnetic field should also be continuous at $r=a$, so that from (2.7), we obtain

$$\begin{aligned}\bar{P}_0&=P_0\frac{a^2}{\varepsilon^2}\left[\frac{1}{2}-\frac{(a-\varepsilon)^2}{a^2}\ln\frac{a}{a-\varepsilon}-\frac{(a-\varepsilon)^2}{2a^2}\right]\\&=P_0[1+\mathrm{O}(\varepsilon/a)]\approx P_0.\end{aligned}$$

3. Governing equations

The linearized MHD equations for compressible plasmas are

$$\frac{\partial\rho_1}{\partial t}+\rho_0(r)\nabla\cdot\boldsymbol{V}_1+\boldsymbol{V}_0\cdot\nabla\rho_1+\boldsymbol{V}_1\cdot\nabla\rho_0(r)=0, \tag{3.1}$$

$$\begin{aligned}&\rho_0(r)\frac{\partial\boldsymbol{V}_1}{\partial t}+\rho_0(r)(\boldsymbol{V}_0\cdot\nabla)\boldsymbol{V}_1\\&=-\nabla P_1+\frac{1}{\mu_0}((\nabla\times\boldsymbol{B}_1)\times\boldsymbol{B}_0+(\nabla\times\boldsymbol{B}_0)\times\boldsymbol{B}_1)+v\nabla^2\boldsymbol{V}_1,\end{aligned} \tag{3.2}$$

$$\frac{\partial\boldsymbol{B}_1}{\partial t}=\nabla\times(\boldsymbol{V}_1\times\boldsymbol{B}_0)+\nabla\times(\boldsymbol{V}_0\times\boldsymbol{B}_1)+\eta\nabla^2\boldsymbol{B}_1, \tag{3.3}$$

$$P_1=c_s^2\rho_1, \tag{3.4}$$

where the subscript "0" denote the initial equilibrium quantities and "1" denote the perturbed quantities, $c_s=(\gamma P_0/\rho_0)^{1/2}$ the sound speed, and γ the adiabatic coefficient. The perturbations are in the form $f_1(r,\theta,z,t)=\tilde{f}_1(r,t)\exp[i(kz+m\theta)]$.

In the vacuum regions, the perturbed magnetic field satisfies $\nabla\times\boldsymbol{B}_1=0$ and $\nabla\cdot\boldsymbol{B}_1=0$, and can therefore be represented by the magnetic flux ψ, or

$$\boldsymbol{B}_1^V=\nabla\psi, \tag{3.5}$$

where ψ satisfies

$$\frac{1}{r}\frac{\partial}{\partial r}\left(r\frac{\partial\psi}{\partial r}\right)-\left(k^2+\frac{m^2}{r^2}\right)\psi=0. \tag{3.6}$$

In the numerical calculations, the variables are normalized by the plasma radius a, the uniform density ρ_0, and the axial magnetic field $B_{0z}=B_0$. The flow velocity is normalized by the Alfvén speed $V_A=B_0/\sqrt{\mu_0\rho_0}$, the time by the Alfvén time $\tau_A=a/V_A$, and the magnetic flux by B_0a. The normalized viscosity coefficient and resistivity are both taken to be 10^{-4}. These contribute to the stability and speed of the numerical calculation.

4. Boundary conditions

The boundary conditions connect the fields in the internal plasma and vacuum regions to the wall. The boundary condition on the plasma–vacuum interface is [23],

$$\begin{aligned}&\left[p_1+B_{0\theta}^pB_{1\theta}^p/\mu_0+B_{0z}^pB_{1z}^p/\mu_0\right]_{r=a-0}\\&\quad-\left[B_{0\theta}^VB_{1\theta}^V/\mu_0+B_{0z}^VB_{1\theta}^V/\mu_0\right]_{r=a+0}\\&=\frac{\xi_r}{2\mu_0}\left(\left[\frac{\partial\left(B_{0\theta}^V\right)^2}{\partial r}\right]_{r=a+0}-\left[\frac{\partial\left(B_{0\theta}^p\right)^2}{\partial r}\right]_{r=a-0}\right),\end{aligned} \tag{4.1}$$

where ξ_r is the radial displacement of the plasma fluid. A second boundary condition at this interface is the continuity of the tangential electric field, or

$$B_{1r}^V=i\left(B_{0\theta}^Vm/r+kB_{0z}^V\right)\xi_r. \tag{4.2}$$

Substituting (4.2) into (4.1) we obtain

$$\begin{aligned}&\left[p_1+B_{0\theta}^pB_{1\theta}^p/\mu_0+B_{0z}^pB_{1z}^p/\mu_0\right]_{r=a-0}\\&\quad-\left[B_{0\theta}^VB_{1\theta}^V/\mu_0+B_{0z}^VB_{1\theta}^V/\mu_0\right]_{r=a+0}\end{aligned}$$

https://doi.org/10.1017/S0022377812000104 Published online by Cambridge University Press

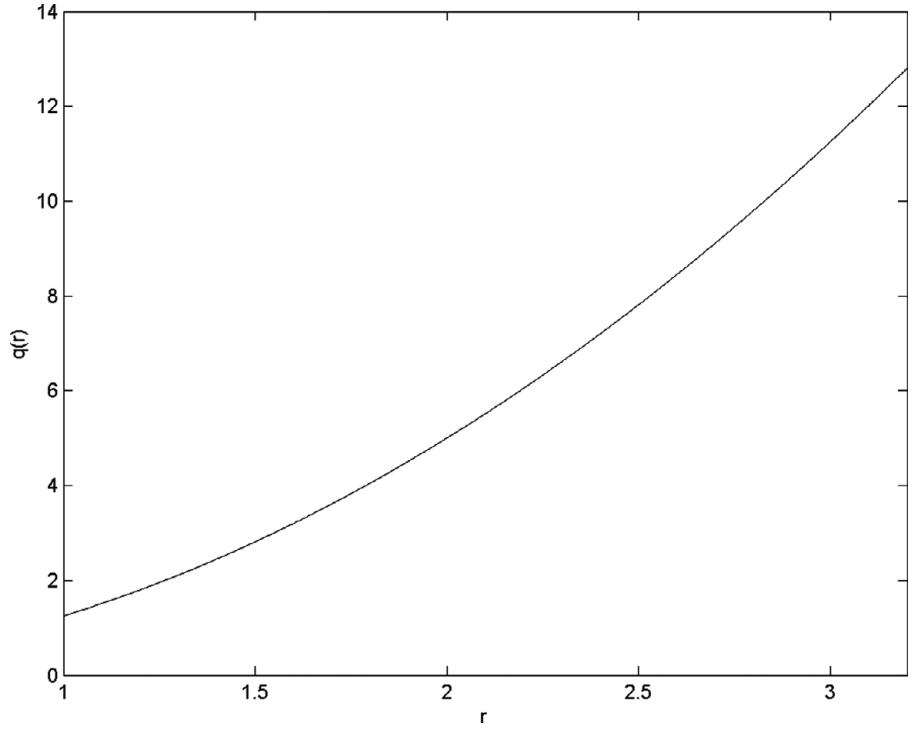


Figure 3. Safety factor $q(r)$ distribution outside the surface current.

$$= \frac{iB_{1r}}{2\mu_0\left(mB_{0\theta}^V/r + kB_{0z}^V\right)}\left(\left[\frac{\partial\left(B_{0\theta}^p\right)^2}{\partial r}\right]_{r=a-0} - \left[\frac{\partial\left(B_{0\theta}^V\right)^2}{\partial r}\right]_{r=a+0}\right) \tag{4.3}$$

for the interface. On the resistive wall, using the thin wall approximation, we have

$$\left.\frac{d\psi}{dr}\right|_{b+\delta} - \left.\frac{d\psi}{dr}\right|_{b} = \frac{1}{c_w}\frac{\partial\psi}{\partial t}, \tag{4.4}$$

where $c_w \equiv (\sigma\mu_0\delta)^{-1}$ is the wall penetration speed with δ the wall thickness and σ is the wall conductivity. At $r = 0$ the usual symmetry condition is used, and at the outer boundary $r = c$ the null boundary condition is used.

5. Numerical results and discussions

The set of equations including the boundary conditions is solved numerically as an initial value problem. In the evaluation, the time step is $\Delta t = 10^{-4}$ and the radial space step is $\Delta r = 10^{-3}$. An initial seed perturbation, namely $B_{1z} = \zeta \exp[-(r-\tilde{r})^2/\lambda^2]$ of small magnitude $\zeta = 10^{-4}$ is applied to trigger the instability. Here, $\tilde{r}$ is the radial location and $\lambda \ll 1$ is the width of the seed perturbation. To model magnetic confinement plasmas where the RWM can appear, an initial uniform axial plasma flow $V_0\hat{z}$ is applied. For simplicity, we assumed that this flow does not affect the initial pressure balance [22], otherwise V_0 is not arbitrary and would be related to P_0 and ρ_0 through the pressure balance condition.

The simulation parameters are as follows. The lengths (see Fig. 1) scaled by the plasma radius are $a = 1.0$, $b = 1.2$, and $c = 2.0$. To model a toroidal plasma, we apply a periodic boundary condition in the axial direction: $\tilde{f}(z) = \tilde{f}(z + 2\pi R_0)$ with $\tilde{f}$ an arbitrary perturbation of the initial equilibrium and $R_0 = 4.0$. This leads to the toroidal mode number $n = kR_0 = 4k$. The other parameters are $\alpha \equiv \beta_0^{1/2} = \mu_0 J_0 a/B_0 = 0.2$, or $\beta_0 \equiv 2\mu_0 P_0/B_{0z}^2 = 0.04$, the sound speed $c_s = \sqrt{\beta_0/2} \approx 0.14$, and the boundary safety factor at the plasma–vacuum interface $q_a = aB_{0z}/R_0 B_{0\theta}(a) = q_{a0}/(1 - 2\varepsilon/a)$, where $q_{a0} = 1.25$, and we recall that the δ-function current corresponds to $\varepsilon \to 0$.

We first consider the stability of MHD modes without the plasma flow. Since in the plasma region, the safety factor $q(r < a - \varepsilon) \to \infty$, the internal mode should be stable. The typical safety factor $q(r)$ outside the surface current is given in Fig. 3. One sees that $q(r)$ outside of the plasma increases monotonously from the boundary value q_a. From the MHD energy principle, the stability condition for the $m = 1$ external kink mode is $q(a) = q_a > 1/n$. For $q_{a0} = 1.25$, all $m = 1$ external modes are thus stable for the present $q(r)$ profile. For the $m \geqslant 2$ external modes, instability occurs only in the narrow window $Y \leqslant q(a) \leqslant m/n$, where $Y \leqslant m/n$ is a number determined by m/n and the current profile $J(r)$. A sharp current profile can therefore stabilize the mode and a

https://doi.org/10.1017/S0022377812000104 Published online by Cambridge University Press

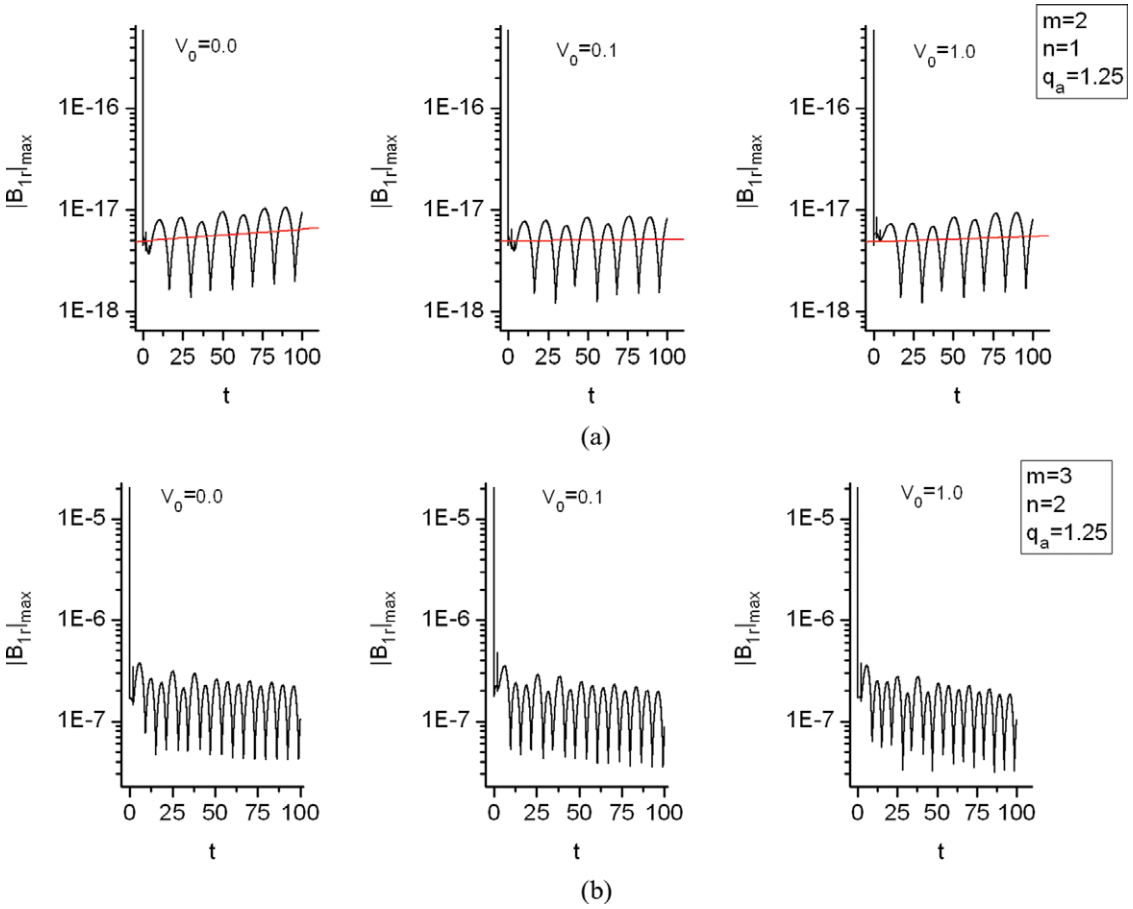


Figure 4. (Colour online) Evolution of the external modes (a) $m/n = 2/1$, and (b) $m/n = 3/2$ for different plasma flow velocities and δ-function surface current distribution.

flat profile can destabilize it. For the surface currents considered here, the modes are stable. The question is then if a flow in the plasma can destabilize the modes?

5.1. *Case I: δ-function surface current distribution*

We first consider the internal mode. Accordingly, the initial seed perturbation is placed in the plasma region, for example, $\tilde{r} = 0.5$ for different initial plasma flow velocities. The radial magnetic field perturbation evolves with time. As expected, the modes only oscillate, with no evidence of growth.

In general, the most unstable external modes in the static equilibrium are $m = 2$ modes. Thus, we first test the $m/n = 2/1$ mode, with $m = 2$, $k = n/4 = 0.25$ and the initial seed perturbation on the $q(r) = 2$ surface in the vacuum region. As seen in Fig. 4(a), there are radial field oscillations with very small magnitude (less than 10^{-17}). For the static case, a slow growth is shown, though not clearly. With the flow, however, the mode is more stable. Thus, the flow has stabilizing effect on the mode [8–18].

The $m/n = 3/2$ external mode is also considered, and it is found that the mode is slowly damped, as shown in Fig. 4(b). Again, the plasma flow has a stabilizing effect on the mode, even for very fast (Alfvénic) flow speeds.

5.2. *Case II: Step-function surface current distribution*

For step-function current distributions with $\varepsilon = 0.001$, 0.01, and 0.1, the safety factor $q(r)$ decreases monotonously inside of the current region from infinity in the plasma to 1.25 at the vacuum–current interface. One might expect certain internal modes to grow in the current region, and the stability property in the current-free plasma region and the vacuum region is similar to Case I.

Since there is no $m/n = 1/1$ rational surface in the current region, we then first test the possible most unstable internal $m/n = 2/1$ mode, again for $m = 2$ and $k = n/4 = 0.25$, but the initial seed perturbation is on the $q(r) = 2$ rational surface of the very thin current region. The result for the $V_0 = 0.0$ static case is shown in Fig. 5(a). It is found that for a very thin current, *e.g.* with thickness $\varepsilon = 0.001$, the mode is very similar to the corresponding $m/n = 2/1$ mode for the δ-function current case, namely with very slow growth. However, finite thickness of the current, *e.g.* $\varepsilon = 0.01$ and $\varepsilon = 0.1$, has a stabilizing effect on the mode. The effect of the flow is considered for the subsonic regime $V_0 = 0.1$ as well as the Alfvén regime $V_0 = 1.0$. The results are shown in Figs. 5(b) and (c). Comparing the results for a wide range (from subsonic to Alfvénic) of flow velocities with that of the static case, we can conclude from Fig. 5(a)

https://doi.org/10.1017/S0022377812000104 Published online by Cambridge University Press

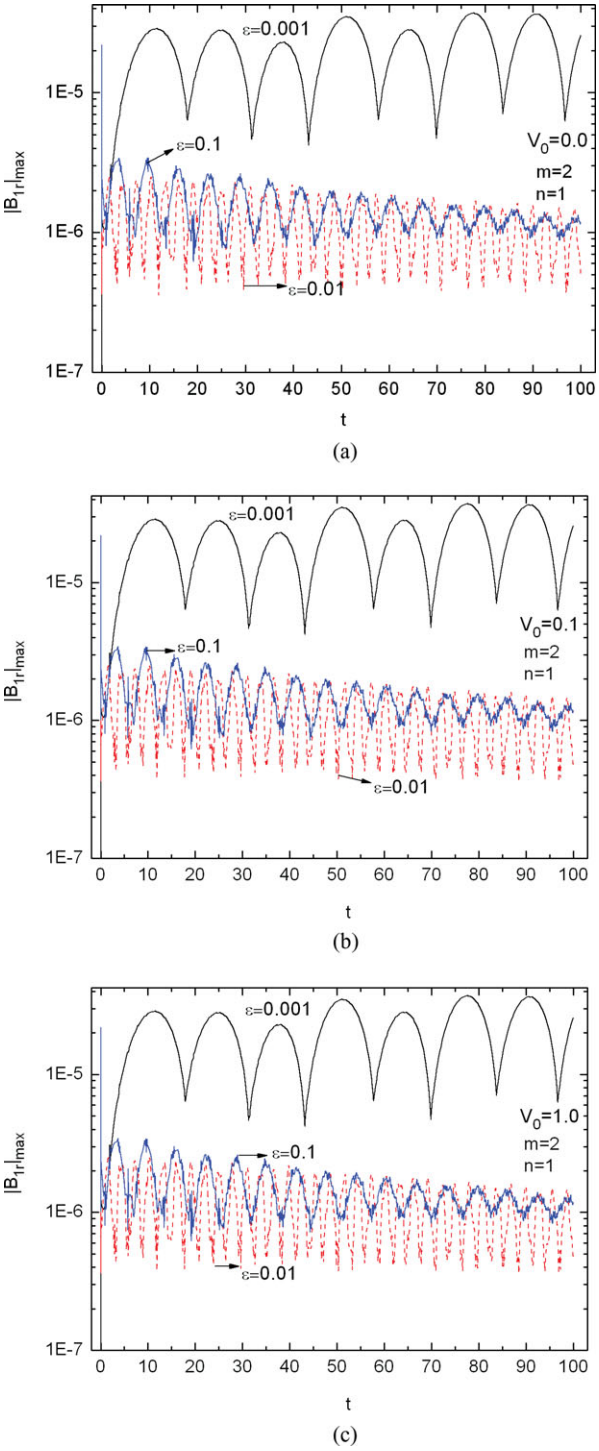


Figure 5. (Colour online) Evolution of the internal $m/n = 2/1$ mode for different surface current thickness and initial flow velocities (a) $V_0 = 0.0$, (b) $V_0 = 0.1$, and (c) $V_0 = 1.0$.

that the plasma flow does not significantly affect the $m/n = 2/1$ RWM. This can be attributed to the fact that the plasma is compressible and our governing equations are linear. In fact, further increase of the flow velocity also does not seem to affect the RWM, although other plasma behavior can be excited.

We have also investigated the other modes, such as the internal $m/n = 3/2$ mode and the external $m/n = 2/1$ and $m/n = 3/2$ modes. The results are qualitatively similar to that of the internal $m/n = 2/1$ mode.

6. Conclusion

In summary, we have investigated the RWMs in a compressible cylindrical plasma in the presence of plasma flow and surface current. It is found that, in contrast to that for an incompressible plasma, both currents have strong stabilizing effects on the internal as well as the external MHD modes.

It should be pointed out that in this work the MHD approximation has been used and higher frequency and/or nonlinear surface perturbations [24, 25] are precluded. The latter are usually unstable and can lead to background turbulence and nonlinear surface structures that can in turn affect the MHD stability [2]. We also have not taken into consideration inhomogeneities in the bulk plasma density and flow, which is expected to affect the RWMs [25, 26].

Acknowledgments

This work is supported by NSFC (11105065), Promotive Research Fund for Excellent Young and Middle-Aged Scientists of Shandong Province (BS2010NJ003) and Science Fund of Ludong University (LY20082704), as well as the National Basic Research Program of China Grant 2008CB717801, 2008CB787103 and 2009GB105004.

References

[1] Aymar, R., Barabaschi, P. and Shimomura, Y. 2002 *Plasma Phys. Control. Fusion* **44**, 519.
[2] Troyon, F., Gruber, R., Saurenmann, H., Semenzato, S. and Succi, S. 1989 *Plasma Phys. Control. Fusion* **26**, 209.
[3] Pfirsch, D. and Tasso, H. 1971 *Nucl. Fusion* **11**, 259.
[4] Jensen, T. H. and Chu, M. S. 1983 *J. Plasma Phys.* **30**, 57.
[5] Gimblett, C. G. 1986 *Nucl. Fusion* **26**, 617.
[6] Freidberg, J. P. 1987 *Ideal Magnetohydrodynamic*. New York: Plenum Press.
[7] Zakharov, L. E. and Putvinskii, S. V. 1987 *Sov. J. Plasma Phys.* **13**, 118.
[8] Bondeson, A. and Ward, D. J. 1994 *Phys. Rev. Lett.* **72**, 2709.
[9] Ward, D. J. and Bondeson, A. 1995 *Phys. Plasmas* **2**, 1570.
[10] Betti, R. and Freidberg, J. P. 1995 *Phys. Rev. Lett.* **74**, 2949.
[11] Boozer, A. H. 1995 *Phys. Plasmas* **2**, 4521.
[12] Fitzpatrick, R. and Aydemir, A. 1996 *Nucl. Fusion* **36**, 11.
[13] Gimblett, C. G., Hastie, R. J., van der Linden, R. A. M. and Wesson, J. A. 1996 *Phys. Plasmas* **3**, 3619.
[14] Fitzpatrick, R. and Jensen, T. H. 1996 *Phys. Plasmas* **3**, 2641.
[15] Bondeson, A. and Xie, X. H. 1997 *Phys. Plasmas* **4**, 2081.
[16] Freidberg, J. P. and Betti, R. 2001 *Phys. Plasmas* **8**, 383.
[17] Finn, J. M. and Chacon, L. 2004 *Phys. Plasmas* **11**, 1866.
[18] Wesson, J. A. 1998 *Phys. Plasmas* **5**, 3816.

https://doi.org/10.1017/S0022377812000104 Published online by Cambridge University Press

[19] Paz-Soldan, C. M., Brookhart, I., Eckhart, A. T., Hannum, D. A., Hegna, C. C., Sarff, J. S. and Forest, C. B. 2011 *Phys. Rev. Lett*. **107**, 245001.

[20] Lashmore-Davies, C. N., Wesson, J. A. and Gimblett, C. G. 1999 *Phys. Plasmas* **6**, 3990.

[21] Cui, S. Y., Wang, X. G., Liu, Y. and Yu, B. 2006 *Phys. Plasmas* **13**, 094506.

[22] Lashmore-Davies, C. N. 2001 *Phys. Plasmas* **8**, 151.

[23] Hasegawa, A. 1975 *Plasma Instabilities and Nonlinear Effects*. Berlin, Heidelberg, New York: Springer-Verlag.

[24] Zhelyazkov, I. and Yu, M. Y. 1978 *J. Plasma Phys*. **20**, 183.

[25] Girka, V. O., Girka, I. O., Girka, A. V. and Pavlenko, I. V. 2011 *J. Plasma Phys*. **77**, 493.

[26] Leonovich, A. S. 2011 *J. Plasma Phys*. **77**, 315.

https://doi.org/10.1017/S0022377812000104 Published online by Cambridge University Press